JOURNAL OF MATERIALS SCIENCE: MATERIALS IN MEDICINE 2 (1991) 19–26

Electrochemistry of AISI 316L stainless steel in calcium phosphate and protein solutions

S. R. SOUSA, M. A. BARBOSA
Department of Metallurgy, Faculty of Engineering, University of Oporto, Rua dos Bragas, 4099 Porto Codex, Portugal

The influence of calcium phosphate and serum on the corrosion resistance of AISI 316L stainless steel in 0.9% NaCl solution was investigated. Both substances are responsible for an increase in the pitting corrosion resistance. Calcium phosphate accelerates the rate of film formation, enhances the release of iron and nickel, and retards that of chromium from a corroding surface. Proteins induce the incorporation of phosphorus and calcium in corrosion products. These effects appear to replicate the accumulation of the same elements observed on stainless steels corroded *in vivo*.

1. Introduction

Electrochemical techniques have been widely employed in accelerated corrosion studies, both *in vivo* and *in vitro*. Their use *in vivo* is related to the measurement of corrosion rates [1, 2] or as a means of introducing metal ions into tissues by the passing of an electrical anodic current [3]. *In vitro* testing has been conducted with the aim of ranking various metals and alloys according to their corrosion resistance [4, 5], studying coated metals [6–8] and the behaviour of dissimilar materials in galvanic couples [9–11], and predicting biocompatibility [12].

To carry out laboratory electrochemical tests the solutions used are normally much less complex than the extracellular fluid contacting with implant materials. Since chloride ions are the most aggressive species existing in the body, test media are essentially chloride solutions with additions of other species. This simplification of the solution chemistry may cause discrepancies between *in vivo* and *in vitro* corrosion behaviour, such as those reported by some authors [1, 13].

Organic species (e.g. proteins) appear to play a fundamental role in metal dissolution [14]. Their inclusion in test media enable more realistic data to be obtained and give an insight into the mechanisms of *in vivo* corrosion.

Strong adsorption to the metal surface appears to be a necessary prerequisite for corrosion inhibition by organic substances. The existence of unfilled orbitals in transition metals and of lone electron pairs on nitrogen and sulphur atoms in protein molecules favours chemisorption. However, this process in itself does not explain corrosion inhibition. In addition, the adsorbed species must possess strongly hydrophobic groups [15]. In contrast, when the organic substance renders the metal surface more hydrophilic the corrosion rate should increase. According to this reasoning the increase in the contact angle at the copper–solution–air interface when albumin is added [16] should be associated with an increase in the corrosion rate, which is exactly what is found [14].

When the metal has a great tendency to react with oxygen, a stable oxide film forms, passivating the surface and preventing direct contact between the metal and the protein. This would be the normal situation with stainless steel, titanium and Co–Cr alloys. The metal–protein bond would be weaker than the metal–oxygen bond, and a decisive influence of proteins on the corrosion rate is not expected. Although no effect on the corrosion rate has been reported for Ti6Al4V [17] and titanium [14], acceleration for stainless steel [17, 18] and c.p. titanium [17], and inhibition for stainless steel [3] have been found. Under fretting the corrosion rate of stainless steel decreased [17, 19, 20], that of c.p. titanium was either accelerated [20] or unchanged [17], and that of Ti6Al4V was not affected [17, 20].

The conflict between the above results is probably merely a consequence of differences in surface states, since the film composition and the charge distribution are bound to influence protein adsorption. For instance, considerable composition changes occur with stainless steels, the surface of which is normally depleted in iron, causing nickel and chromium enrichment [9]. Molybdenum is also depleted [21]. Fretting in albumin solutions produces selective dissolution of nickel [19]. Since nickel has a minor influence on the corrosion resistance of stainless steels, its removal would not lower their corrosion resistance, but would cause exactly the opposite effect due to chromium enrichment. The process of nickel removal by proteins has not been clarified, but its presence in the oxide film as a non-oxidized element [22, 23] could facilitate complex formation with proteins.

The foregoing aspects are only part of the complex behaviour of metals in physiological media. Among other species, calcium and phosphate ions may also have an effect on the electrochemical process of dis-

0022–2461/91 $03.00 + .12

solution occurring on a metal surface, but their role has not been considered in accelerated *in vitro* testing. A programme of studies has therefore been conducted to establish the influence of these ions on the electrochemical behaviour of stainless steel and titanium in physiological media, in the presence and in the absence of proteins.

In this paper the effect of these species on corrosion susceptibility is analysed under static conditions for AISI 316L stainless steel in isotonic 0.9% NaCl solution. The research involved the use of conventional potentiostatic experiments, aimed at measuring corrosion currents in the passive state and the breakdown potentials. Galvanostatic polarization and film formation kinetics experiments were also performed. Although not commonly used in biomaterials research, both techniques can provide useful information about the electrochemical characteristics of passive surfaces. In galvanostatic tests the maximum potential attained by the electrode can be regarded as the breakdown or pitting potential, E_p. After E_p being attained E_p the potential drops and tends to stabilize at a value corresponding to the protection potential, E_{prot} [24]. The kinetics of passivation can be evaluated by the transient currents produced upon instantaneous application of a potential in the passive region. The technique relies on the assumption that the faster the current decreases, the more rapidly film formation takes place [25–27].

2. Materials and methods

AISI 316L stainless steel specimens, 1.0 mm thick, with an area of 880 mm^2, were used. In order to avoid crevice corrosion, samples with the configuration shown in Fig. 1 were employed. They were wet-ground with SiC papers down to 600 grit and washed with deionized water in an ultrasonic bath for 3 min. They were then immersed in a solution of 20% HF + 20% HNO_3 (v/v) for 6 min, at room temperature, and washed with water in an ultrasonic bath for 3 min. They were then passivated in a solution of 30% HNO_3 (v/v) at 60 °C for 30 min, thoroughly washed in deionized water, rinsed in alcohol and dried. The electrical contact was made by winding an electrical wire (diameter 0.5 mm) to the end of the electrode. This connection was painted with coloidal silver, covered with polytetrafluoroethylene tape and with protective lacquer (Lacomit), as shown in Fig. 1.

The square area of the electrodes was immersed in solutions of various compositions (Table I). Solutions were prepared by the method described by Cheng [28]. Solutions with calcium and phosphate were prepared at 37 ± 1 °C, by mixing equal volumes of two solutions, one containing $CaCl_2$ and NaCl, and the other Na_2HPO_4 and NaCl. Bovine serum (Difco) was added to the first solution. The pH was adjusted to 7.40 ± 0.05, with 1.0 M HCl. All solutions were prepared with distilled and deionized water. The chemical reagents were of p.a. grade. Using a thermostatic bath, solutions were kept at 37 ± 1 °C. They were de-aerated with nitrogen U for at least 150 min before the tests and magnetically stirred.

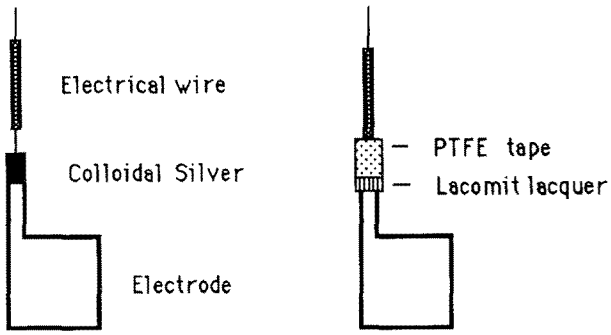

Figure 1 Schematic representation of the electrical connection to the samples (left) and protection of the connecting area (right).

TABLE I Composition of solutions used and their designation

Designation	Composition
NaCl	NaCl 0.154 M
NaCl + Ca + P	NaCl 0.154 M, $CaCl_2$ 1.0 mM, Na_2HPO_4 2.7 mM
NaCl + Ca + P + serum	NaCl 0.154 M, $CaCl_2$ 1.0 mM, Na_2HPO_4 2.7 mM, 10% bovine serum (Difco)

The electrochemical cell was made of metilpenthen polymer and its capacity was 200 ml. A saturated calomel electrode (SCE) was used as the reference electrode. In potentiostatic experiments the auxiliary electrode was a platinum square sheet of area 800 mm^2. In galvanostatic experiments an auxiliary electrode identical to the working electrode, but non-passivated, was used.

A potentiostat–galvanostat was used for application of potential and current. In potentiodynamic tests the potential sweep rate was 100 mV min^{-1}, starting from the corrosion potential and going up to 1000 mV. In potentiostatic experiments 400 and 500 mV were applied. In galvanostatic experiments the current density applied was 1.14 mA cm^{-2}. Before switching on the potentiostat-galvanostat the specimens were left under open circuit for 10 min.

A computer and a multiplexer unit were used for potential and current data acquisition. The data were recorded at 1 sec intervals. Chemical analysis of solutions and precipitates was done by atomic absorption spectroscopy (AAS), using flame or electrothermal atomization (EA) in a graphite furnace. Attack morphologies were observed in a scanning electron microscope (SEM) and the corrosion products analysed semiquantitatively by energy-dispersive X-ray analysis.

3. Results

Fig. 2 shows a typical E–t curve obtained by the galvanostatic method. Initially, the potential increases due to film thickening under the action of the electrical field. When the critical potential for film breakdown, E_p, is attained, the film is locally destroyed and pitting starts. Pit initiation is accompanied by a potential drop caused by the localized disappearance of the passive film, across which most of the total potential difference between solution and metal occurred. The

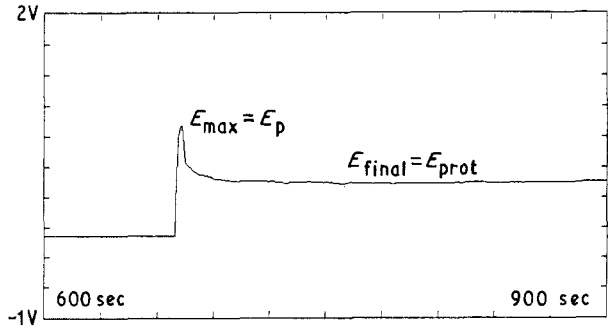

Figure 2 Galvanostatic curve for AISI 316L stainless steel immersed in NaCl solution.

potential oscillations observed after the peak correspond to activation (potential drops) and repassivation (potential increases) events.

In this region the electrode is maintained in a state of partial activation, since the growth of some pits requires repassivation of others for the total current to remain constant. The final potential attained in the tests has been used as the protection potential, E_{prot}.

Table II gives the most significant parameters that can be taken from curves similar to that in Fig. 2. The cathode and anode potentials measured immediately before application of the current ($t=0$) are the corrosion potentials, E_{corr}. The corrosion potential of the cathode is always significantly lower than that for the anode because the former was used in the as-ground state, without passivation in nitric acid solution. This enables a comparison of the influence of calcium phosphate solutions and of serum additions on the E_{corr} of non-passivated specimens (E_{cath}). A 90 mV decrease occurs when calcium and phosphate ions are added to the initial NaCl solution, but a much larger drop (about 460 mV) is observed upon adding serum. A similar trend towards active potential values occurs with the passivated electrodes (E_{an}), although less significant. The tendency of these electrodes to resist activation can be associated with the higher stability of their surfaces introduced by the nitric acid treatment.

The maximum potential reached in these tests (E_{max}) provides evidence for a beneficial influence of calcium and phosphate ions and serum on the resistance of the film to attack by chloride ions. Calcium and phosphate ions increase E_{max} by about 140 mV. When serum is added a further increase in E_{max}, of the order of 500 mV, occurs. The time for breakdown, t_{br}, is also largest when serum is present. An intermediate time is obtained for calcium and phosphate additions, t_{br} and E_{max} are naturally related, since higher potentials should be reached after longer times.

When the protection potentials are compared (E_{an} at $t = t_f$ in Table II), the trends reported above are confirmed, i.e. calcium phosphate and calcium phosphate + serum solutions provide increasingly higher degrees of protection.

The anodic polarization curves shown in Fig. 3 do not provide a discrimination between the behaviour of the stainless steel in the various solutions as clearly as the galvanostatic tests. There is practically no difference in the passive current densities. Once pitting starts, the rise in current is steepest for the simple saline solution and flattest for the calcium phosphate + serum solution. This is indicative of an inhibitory effect of serum in the propagation stage of pitting. Fig. 3 shows that calcium phosphate solutions act in a similar way. Table III gives the pitting potentials obtained in the three media. In calcium phosphate solutions the pitting potential is about 170 mV higher than in simple 0.9% NaCl solution, but 50 mV lower than in calcium phosphate + serum solution. This difference is within the limits of experimental error, and therefore no special significance should be attached to it. The trends in these potentiodynamic tests, although confirming the general tendency obtained in the galvanostatic experiments, are less clear. The greater discriminating power of the latter technique justifies it being applied more often.

In potentiostatic experiments at 400 and 500 mV current decay curves were used to evaluate the process of film formation. Figs 4 and 5 show curves obtained at 400 and 500 mV, respectively. At neutral pH and during the initial film formation process it may be considered that these currents are used in forming a passive layer, and that only a small fraction corresponds to metal cations that go into solution [26, 27, 29, 30]. The charge consumed in building up this layer is shown in Figs 6 and 7 for $E = 400$ mV and $E = 500$ mV, respectively. These figures show that film formation in the simple saline solution consumes less charge than in the other two solutions. By Faraday's law the charge is proportional to the film thickness, and therefore what Figs 6 and 7 show is that in

TABLE II Electrochemical data for 316L stainless steel obtained in galvanostatic experiments

Surface treatment	Solution	$t=0$[a]		$t=t_f$[b]		E_{max}[c] (V)	t_{br}[d] (sec)
		E_{cath} (V)	E_{an} (V)	E_{cath} (V)	E_{an} (V)		
Passivation	NaCl	− 0.249	− 0.126	− 1.248	0.230	0.755	1
Passivation	NaCl + Ca + P	− 0.339	− 0.187	− 1.312	0.295	0.891	3
Passivation	NaCl + Ca + P + serum	− 0.713	− 0.331	− 1.417	0.323	1.397	17

[a] $t=0$: application of current density of 1.14 mA cm^{-2}. E_{cath} and E_{an} are, respectively, the cathode and the anode corrosion potentials immediately before galvanostatic polarization.
[b] $t=t_f$: end of test. E_{an} is the protection potential.
[c] E_{max} is the pitting potential.
[d] t_{br} is the time at which E_{max} is reached.

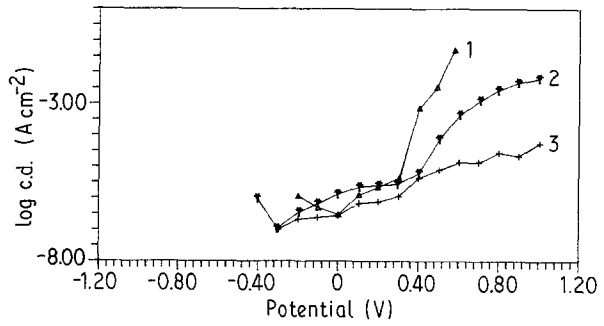

Figure 3 Anodic polarization curves in (1) NaCl, (2) NaCl + Ca + P and (3) NaCl + Ca + P + serum.

TABLE III Pitting potentials of AISI 316L stainless steel in different solutions

Solution	Pitting potential (mV)
NaCl	333 ± 58
NaCl + Ca + P	500 ± 141
NaCl + Ca + P + serum	550 ± 71

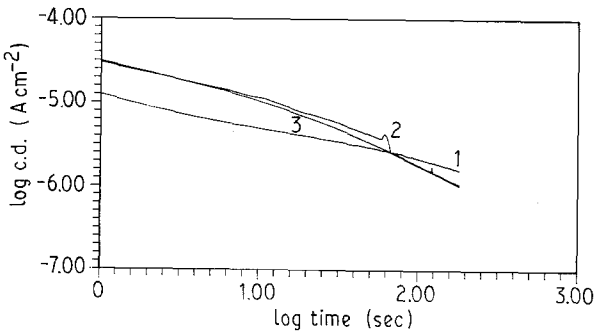

Figure 4 Log c.d. against log time curves obtained by potentiostatic method at 400 mV in (1) NaCl, (2) NaCl + Ca + P and (3) NaCl + Ca + P + serum.

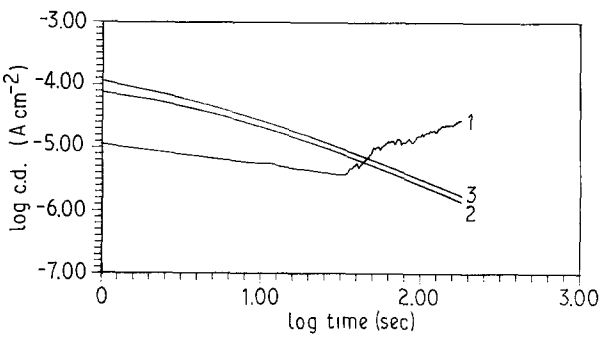

Figure 5 Log c.d. versus log time curves obtained by potentiostatic method at 500 mV in (1) NaCl, (2) NaCl + Ca + P and (3) NaCl + Ca + P + serum.

calcium phosphate and calcium phosphate + serum solutions the passive layer should be thicker than in simple saline solutions. Auger electron spectroscopy (AES) of films formed on stainless steel *in vivo* and *in vitro* provide direct evidence for this film thickening process [21]. The authors report that proteins produced thicker layers than simple isotonic solutions.

The charge transients have been fitted to an expression of the form

$$Q = k_1 + k_0 \ln(t + \tau) \quad (1)$$

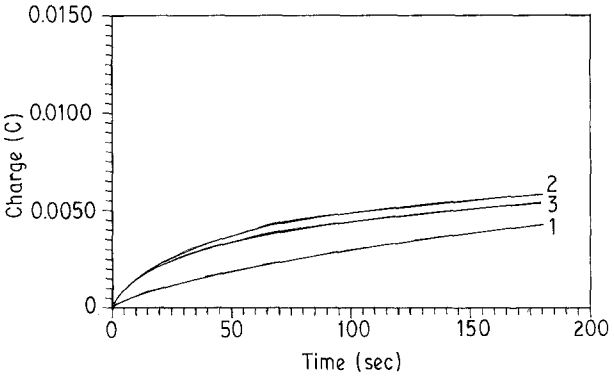

Figure 6 Charge consumed in building up the passive layer at 400 mV in (1) NaCl, (2) NaCl + Ca + P and (3) NaCl + Ca + P + serum.

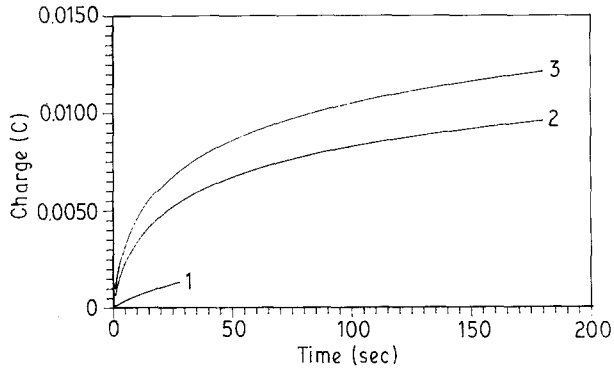

Figure 7 Charge consumed in building up the passive layer at 500 mV in (1) NaCl, (2) NaCl + Ca + P and (3) NaCl + Ca + P + serum.

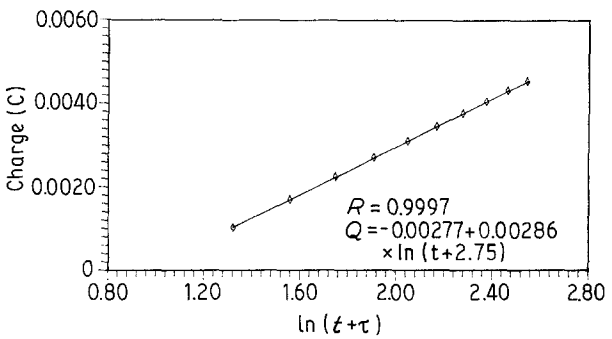

Figure 8 Example of charge against ln(t + τ) curves; NaCl + Ca + P + serum; E = 500 mV.

where k_1, k_0 and τ are constants. This is the direct logarithmic law of film growth [31], corresponding to the place-exchange mechanism [32]. The constants were calculated by appropriate computer software that minimizes the sum of deviation-squares. Fig. 8 gives an example of the Q against $\ln(t + \tau)$ curves. Nearly perfect correlations were always obtained. Table IV indicates the values of k_0, k_1 and τ, as well as the charge at 10 sec, Q_{10}. The influence of calcium phosphate and serum additions on film growth can be analysed with the help of k_0 and Q_{10}. k_0 indicates the rate of film growth, whereas Q_{10} is a measure of film thickness. For each solution film growth is faster at 500 mV than at 400 mV, as concluded from the k_0 values. The films at 500 mV should also be thicker than at 400 mV, as indicated by the Q_{10} values.

TABLE IV Constants k_0, k_1 and τ in Equation 1 and charge at $t = 10$ sec

Solution	E (mV)	k_0 (mC)	k_1 (mC)	τ (sec)	Q_{10} (mC)
NaCl	400	0.9	− 2.3	12.4	0.60
NaCl	500	1.6	− 4.1	14.6	0.95
NaCl + Ca + P	400	1.9	− 4.2	9.4	1.5
NaCl + Ca + P	500	2.4	− 2.9	3.4	3.3
NaCl + Ca + P + serum	400	1.4	− 2.6	6.3	1.5
NaCl + Ca + P + serum	500	2.9	− 2.8	2.7	4.5

Calcium phosphate speeds up the film formation kinetics, but serum does not appear to have a similar effect. Calcium phosphate and calcium phosphate + serum solutions produce thicker films than simple saline solutions, as previously pointed out.

4. Discussion

This research shows that there is a clear inhibition of corrosion caused by the presence of calcium and phosphate ions. This effect is manifested in all of the experiments, but the galvanostatic method is the one that provides the clearest evidence, particularly through about 140 and 65 mV shifts in the pitting (maximum) and protection (final) potentials, respectively. The potentiostatic tests gave significantly lower pitting potentials than the galvanostatic technique, which is explained perfectly by the influence of the potential sweep rate, $\Delta E/\Delta t$, on E_p. It has long been recognized that the general tendency is for E_p to increase as $\Delta E/\Delta t$ becomes greater [33, 34], and since Table II shows that the galvanostatic pitting potentials were attained within very short times, their values should be higher than the E_p measured in potentiodynamic experiments. If a linear rate of potential increase is assumed for the galvanostatic tests, then $\Delta E/\Delta t = 360\,\text{mV sec}^{-1}$, a value much higher than that applied potentiodynamically (about $1.7\,\text{mV sec}^{-1}$).

The data are not conclusive as to whether the presence of calcium and phosphate ions interfere only with the properties of the passive film or also with the process of pit propagation. First, it must be considered that the above ions influence the kinetics of film growth and its thickness. The values of k_0 in Table IV indicate that calcium and phosphate speed up film growth, at both 400 and 500 mV. In the same table, Q_{10} shows that the charge consumed increases. The rupture of these films depends on a series of factors, namely their composition, structure and thickness, which may all be influenced by the composition of the medium. A more detailed study of the characteristics of the films is being undertaken, but a discussion based on thickness is consistent with increased breakdown potentials, since thicker films should require higher electrode potentials, assuming that the electrical field strength across them is approximately the same. Secondly, calcium phosphate acts as an inhibitor of pit propagation, since the protection potential increases by 65 mV (Table II), indicating that pit repassivation can occur at more oxidizing potentials when calcium and phosphate ions are present.

The corrosion products covering the pits had a very complex composition. They appeared to contain various amounts of metal chlorides, hydroxides and phosphates. X-ray diffraction of the corrosion products showed them to be amorphous. A comparison between the solubilities of metal chlorides, hydroxides and phosphates would be practically of no value as a means of explaining the formation of these precipitates, owing to great variability in their composition. However, in corrosion products formed in calcium phosphate solutions chloride predominated over phosphate, as Table V shows (P/Cl ratios less than unity). Serum additions had the effect of reversing this trend, a clear predominance of phosphates being now observed, with P/Cl ratios as high as 12 being obtained. Table V also shows that only a small fraction of the total phosphate could be associated to calcium, since the Ca/P ratios were normally lower than for any common phosphate. Most of the phosphate was, therefore, probably associated to the stainless steel elements. It is of interest to note that in the presence of serum the corrosion products were richer in calcium than those formed in calcium phosphate solutions. Another relevant information in Table V is the considerable increase in the Cr/Fe ratio with respect to alloy composition. The corrosion products were often five times richer in chromium than the alloy, for which the Cr/Fe ratio is 0.26. The corrosion products formed in serum solutions also contained considerable amounts of sulphur coming from proteins. The presence of these elements in the corrosion products

TABLE V Energy dispersive analysis of corrosion products (wt %)

Method	Solution	P/Cl	Cr/Fe[a]	Ca/P	S (%)
Galvanostatic	NaCl	0	−	/	< D.L.
	NaCl + Ca + P	< 1	−	[b]	< D.L.
	NaCl + Ca + P + serum	> 1 (max. 5.7)	+ (max. 1.8)	< 0.1	max. 22
Potentiodynamic	NaCl	0	+ (max. 0.8)	/	max. 5
	NaCl + Ca + P	< 1	+ (max. 0.6)	< 0.1	max. 3
	NaCl + Ca + P + serum	> 1 (max. 12.4)	+ (max. 1.3)	> 0.1 (max. 0.4)	max. 29

[a] − denotes ratios smaller than alloy proportions, + denotes ratios greater than alloy proportions.
[b] Both elements were below the detection limit (D.L.: 0.5%).

formed in calcium phosphate + serum solutions has close similarities with the *in vivo* situation. Chlorine, calcium, sulphur and particularly large amounts of phosphorus were found in tissue samples [35, 36]. In both works the metallic element chromium was often present in large proportions.

The precipitates collected at the bottom of the cell contained the same elements detected around the pits. The analyses were done by energy dispersion after washing the precipitates with distilled water six times, in order to eliminate the solute. Calcium and phosphorus were always found. It has not been possible to establish whether precipitation of phosphates occurred only on the metal surface or also in the solution, with the corrosion products fragments detached from the metal acting as heterogeneous nucleation sites. Regardless of these aspects, it has been found that corrosion had the effect of promoting phosphate precipitation. In normal circumstances a solution with 1.0 mM $CaCl_2$, 2.7 mM Na_2HPO_4 and pH 7.4 should remain clear for more than 24 h at 37 °C with stirring [28]. Under galvanostatic control, precipitation started within a few minutes of the application of current, and by the end of the tests (50 min) the calcium content had reached a low level (0.44 mM).

Fig. 9 shows the variation in concentration of iron, chromium, nickel, calcium and phosphorus with time in simple isotonic and calcium phosphate solutions. These determinations were made by AAS (flame and EA). Iron and nickel concentrations increase continuously, whereas chromium shows a maximum and a minimum at 20 and 30 min, respectively. The maximum would be associated with the outset of chromium chloride precipitation. A plausible explanation for the increase that follows after 30 min cannot be found, although acidification due to metal hydrolysis could be a possibility. Fig. 9 also shows that calcium phosphate had an important effect on the concentration of the metallic elements in solution. While nickel and iron concentrations increase, that of chromium decreases. The enhanced dissolution of iron and nickel had the effect of leaving more chromium on the surface, which provides an acceptable explanation for the beneficial influence of calcium phosphate on the corrosion resistance. Analysis of the precipitates collected at the bottom of the cell confirms that nickel and iron dissolution is enhanced by the presence of calcium phosphate, as Table VI shows. The increase for iron (9%) is about twice as much as that for nickel (5%).

Serum added to calcium phosphate solutions had the capacity of improving even further the corrosion resistance of stainless steel. This is particularly evident in the high pitting potential given in Table II. The action of serum can be ascribed to corrosion inhibition caused by proteins, via an adsorption mechanism which can be illustrated by using albumin as an example. Albumin is the protein in highest concentration in normal serum and has been studied in more detail than other proteins. At the pH of the test solutions (7.4) albumin is negatively charged since its isoelectric point is 4.5 [19]. The experimental method used in the present work polarizes the stainless steel

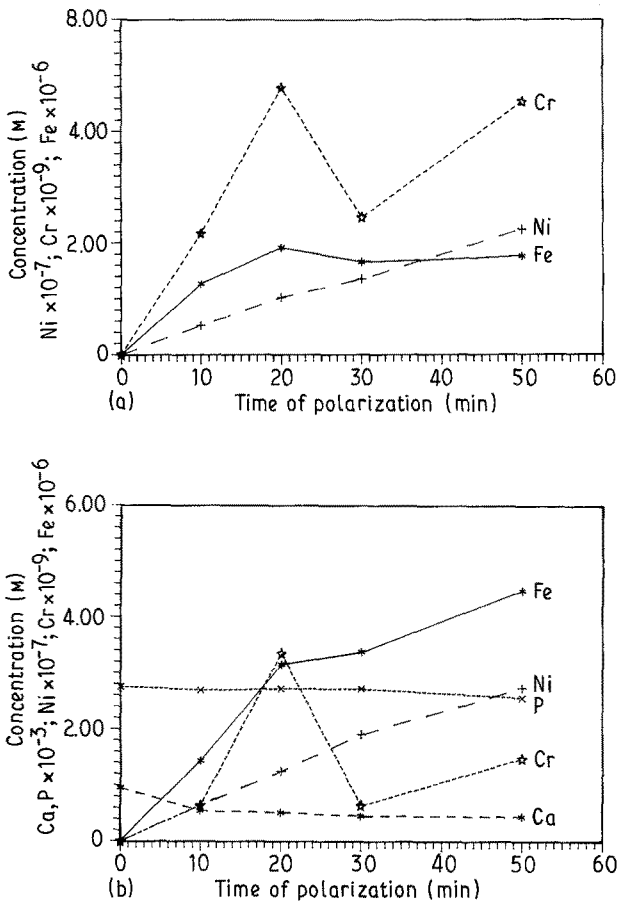

Figure 9 Variation in concentration of Fe, Cr, Ni, Ca and P with time in (a) NaCl and (b) NaCl + Ca + P solutions.

surface in the anodic direction, creating therefore an electron depletion. This favours the adsorption of negatively charged species, and albumin would thus tend to form an adsorbed film. Since chemical and structural heterogeneities on the metal originate variations in the surface charge, albumin would be more easily attracted towards the most positively charged regions, namely those where metal cations are being released. A competition between protein and chloride adsorption would retard the film breakdown caused by the latter ion, thus explaining the higher potentials and longer times for breakdown shown in Table II.

The improvement in pitting corrosion resistance observed in this work is in apparent contradiction with the increase in corrosion rate reported by other researchers [17, 18] who have performed their tests under free corrosion conditions. In strict terms a comparison between both methods of corrosion resistance evaluation is not legitimate, since our method is based on pitting potential and protection potential measurements, and their method consists of corrosion rate determinations. However, under an applied potential of 500 mV the corrosion rate in serum was significantly lower than in saline [3]. This result agrees with the action of serum in our experiments and can be explained by the potential induced adsorption mechanism proposed above. Both works provide support to the idea that proteins inhibit corrosion and that they can be responsible for the lower corrosion rates found *in vivo* than in isotonic saline [1]. The acceleration of corrosion found *in vitro* under open-

TABLE VI Amounts of metallic and non-metallic elements in precipitates. Galvanostatic tests; $i = 1.14\ mA\ cm^{-2}$, $t = 50$ min

Solution	Number of moles				
	Calcium	Phosphorus	Chromium	Nickel	Iron
NaCl			2.25×10^{-5}	15.5×10^{-6}	8.31×10^{-5}
NaCl + Ca + P	3.02×10^{-4}	1.43×10^{-3}	2.26×10^{-5}	16.2×10^{-6}	9.04×10^{-5}

circuit conditions when proteins are added can perhaps be explained by an activation process occurring near the passivation potential, which would be different from the breakdown phenomena that take place at or above the pitting potential. In fact, both in this work and in a work of Brown and Merritt [37] serum causes a decrease in the corrosion potential. This not only renders adsorption of negatively charged proteins more difficult, but could also lead to activation of the electrode. The polarization curves published by the same authors [18] show that serum increased the passivation current, rendering the passive film less stable at the lower end of the passive region.

The differences in film growth kinetics between serum and non-serum calcium phosphate solutions are small compared with those for isotonic saline (Figs 6 and 7 and Table IV). It seems, however, that the charges are slightly higher for films grown in serum. The largest effect is clearly due to calcium phosphate additions. This reflects a distinct role of proteins and calcium phosphate on corrosion inhibition. While proteins appear to act mainly through adsorption, calcium phosphate changes the film growth kinetics.

5. Conclusions

The galvanostatic method is capable of discriminating the influence of calcium phosphate and proteins on the resistance to pitting corrosion better than the potentiodynamic technique.

Calcium phosphate and proteins improve the pitting resistance of stainless steel in 0.9% NaCl solution.

Calcium phosphate accelerates film growth kinetics, whereas proteins have practically no effect.

Calcium phosphate enhances the release of iron and nickel and retards that of chromium from a corroding surface.

Proteins induce the incorporation of phosphorus and calcium in corrosion products.

An enrichment in chromium and presence of calcium and phosphorus in corrosion products similar to those found on stainless steels corroded *in vivo* is produced in electrochemical *in vitro* tests done in calcium phosphate + serum solutions, but not in non-serum solutions.

Acknowledgement

The support of JNICT under contract 908.86.222 is gratefully acknowledged.

References

1. R. W. REVIE and N. D. GREENE, *J. Biomed. Mater. Res.* **3** (1969) 467.
2. S. G. STEINEMANN, in "Titanium, Science and Technology", edited by G. Lutjering, U. Zwicker and W. Bunk, Vol. 2 (Deutsche Gesellschaft für Metallkunde, Oberurse, FRG, 1985) p. 1373.
3. S. A. BROWN, L. J. FARNSWORTH, K. MERRITT and T. D. CROWE, *J. Biomed. Mater. Res.* **22** (1988) 321.
4. A. C. FRAKER, A. W. RUFF, P. SUNG, A. C. VAN ORDEN and K. M. SPECK, in "Titanium Alloys in Surgical Implants" (ASTM STP 796), edited by H. A. Luckey and F. Kubli, Jr (American Society for Testing and Materials, Philadelphia, 1983) p. 206.
5. A. CIGADA, G. RONDELLI, B. VICENTINI, M. GIACOMAZZI and A. ROOS, *J. Biomed. Mater. Res.* **23** (1989) 1087.
6. M. L. ESCUDERO, J. A. GONZALEZ and J. RUIZ, *Werkst. Korros.* **39** (1988) 364.
7. Y. ARATA, A. OHMORI, G.-Q. ZHOU, J. XUE and C.-J. LI, *Trans. Jpn Welding Res. Inst.* **13** (1984) 107.
8. P. DUCHEYNE, *Biomaterials* **4** (1983) 185.
9. R. A. SILVA, M. A. BARBOSA, G. M. JENKINS and I. SUTHERLAND, *Biomaterials*, **11** (1990) 336.
10. C. D. GRIFFIN, R. A. BUCHANAN and J. E. LEMONS, *J. Biomed. Mater. Res.* **17** (1983) 489.
11. N. G. THOMPSON, R. A. BUCHANAN and J. E. LEMONS, *ibid.* **13** (1979) 35.
12. H. ZITTER and H. PLENK, Jr, *ibid.* **21** (1987) 881.
13. M. MORITA, T. SASADA, H. HAYASHI and Y. TSUKAMOTO, *ibid.* **22** (1988) 529.
14. G. C. F. CLARK and D. F. WILLIAMS, *ibid.* **16** (1982) 125.
15. YU. KUZNETSOV, S. V. OLEYNIK, N. N. ANDREEV and S. S. VESELY, in Proceedings, 6th European Symposium on Corrosion Inhibitors, Ann. Univ. Ferrara, N. S., Sez V, Suppl. 8, 1985, p. 567.
16. D. F. WILLIAMS and R. L. WILLIAMS, in "Implant Materials in Biofunction", edited by C. de Putter, G. L. de Lange, K. De Groot and A. J. C. Lee (Advances in Biomaterials, Vol. 8) (Elsevier Science, Amsterdam, 1988) p. 275.
17. R. L. WILLIAMS, S. A. BROWN and K. MERRITT, *Biomaterials* **9** (1988) 181.
18. S. A. BROWN and K. MERRITT, *J. Biomed. Mater. Res.* **14** (1980) 173.
19. K. MERRITT and S. A. BROWN, *ibid.* **22** (1988) 111.
20. S. A. BROWN and K. MERRITT, in "Corrosion and Degradation of Implant Materials: Second Symposium" (ASTM STP 859), edited by A. C. Fraker and C. D. Griffin (American Society for Testing and Materials, Philadelphia, 1985) p. 105.
21. D. D. ZABEL, S. A. BROWN, K. MERRITT and J. H. PAYER, *J. Biomed. Mater. Res.* **22** (1988) 31.
22. J. E. CASTLE and C. R. CLAYTON, *Corros. Sci.* **17** (1977) 7.
23. R. A. SILVA, M. A. BARBOSA, A. M. COSTA, M. DA CUNHA BELO and I. SUTHERLAND, "Clinical Implant Materials", edited by G. Heinke, U. Soltèsz and A. J. C. Lee (Advances in Biomaterials, Vol. 9, Elsevier Science Publishers, BV, Amsterdam, 1990) p. 43.
24. Z. SZKLARSKA-SMIALOWSKA and M. J. CZACHOR, *Corros. Sci.* **11** (1971) 901.
25. M. A. BARBOSA and J. C. SCULLY, *ibid.* **22** (1982) 1025.
26. M. A. BARBOSA, *Corrosion* **43** (1987) 309.
27. *Idem., ibid.* **44** (1988) 149.
28. P. T. CHENG, *Calcif. Tissue Int.* **40** (1987) 339.

29. P. I. MARSHALL and G. T. BURSTEIN, *Corros. Sci.* **23** (1983) 1219.
30. *Idem., ibid.* **24** (1984) 463.
31. C. LUKAC, J. B. LUMSDEN, S. SMIALOWSKA and R. W. STAEHLE, *J. Electrochem. Soc.* **122** (1975) 1571.
32. N. SATO and M. COHEN, *ibid.* **111** (1964) 512.
33. T. SZAUER and J. JACOBS, *Corros. Sci.* **16** (1976) 945.
34. H. P. LECKIE, *J. Electrochem. Soc.* **117** (1970) 1152.
35. H. F. HILDEBRAND, P. OSTAPCZUK, J. F. MERCIER, M. STOEPPLER, B. ROUMAZEILLE and J. DECOULX, in "Biomaterials Degradation – Fundamental Aspects and Related Clinical Phenomena", edited by M. A. Marbosa (Elsevier Science, in press).
36. R. A. SILVA, M. A. BARBOSA, A. S. COSTA and J. A. C. RIBEIRO, Proc. Materiais 85, Vol. 5 (Sociedade Portuguesa de Materiais, Oporto, 1985).
37. S. A. BROWN and K. MERRITT, *J. Biomed. Mater. Res.* **15** (1981) 479.

Received 23 April
and accepted 16 May 1990